Enhanced carbohydrate production by Southern Ocean phytoplankton in response to in situ iron fertilization

van Oijen, T; Veldhuis, MJW; Gorbunov, MY; Nishioka, J; van Leeuwe, Maria; de Baara, HJW; de Baar, Henricus

Published in:
Marine Chemistry

DOI:
10.1016/j.marchem.2004.06.039

Publication date:
2005

Available online at www.sciencedirect.com

SCIENCE DIRECT®

Marine Chemistry 93 (2005) 33–52

MARINE CHEMISTRY

www.elsevier.com/locate/marchem

Enhanced carbohydrate production by Southern Ocean phytoplankton in response to in situ iron fertilization

T. van Oijen[a,*], M.J.W. Veldhuis[b], M.Y. Gorbunov[c], J. Nishioka[d], M.A. van Leeuwe[a], H.J.W. de Baar[a,b]

[a]*University of Groningen, Department Marine Biology, CEES, P.O. Box 14, 9750 AA Haren, The Netherlands*
[b]*Royal Netherlands Institute for Sea Research, P.O. Box 59, 1790 AB Den Burg, Texel, The Netherlands*
[c]*Environmental Biophysics and Molecular Ecology Program, Institute of Marine and Coastal Sciences, Rutgers, The State University of New Jersey, 71 Dudley Road, New Brunswick, NJ 08901, USA*
[d]*Central Research Institute of Electric Power Industry, 1646 Abiko, Abiko, Chiba 270-1194, Japan*

Received 14 August 2003; received in revised form 15 March 2004; accepted 16 June 2004
Available online 7 October 2004

Abstract

Storage carbohydrates (e.g., water-extractable β-1,3-D-glucan in diatoms) are of key importance for phytoplankton growth in a variable light climate, because they facilitate continued growth of the cells in darkness by providing energy and carbon skeletons for protein synthesis. Here, we tested the hypothesis that synthesis of storage carbohydrates by phytoplankton in the Southern Ocean is reduced by low iron and light availability. During the EisenEx/CARbon dioxide Uptake by the Southern Ocean (CARUSO) in situ iron enrichment experiment in the Atlantic sector of the Southern Ocean in November 2000, we studied the dynamics of water-extractable carbohydrates in the particulate fraction over the period of 3 weeks following the iron release. The areal amount (integral between 0- and 100-m depth) of carbohydrates increased from 1400 to 2300 mg m^{-2} inside the iron-enriched patch, while remaining roughly constant in the surrounding waters. Most of the increase inside the patch was associated with the fraction of large (>10 μm) phytoplankton cells, consistent with the shift in the community structure towards larger diatoms. Deck incubations at 60% of the ambient irradiance revealed that the diurnal chlorophyll *a* (Chl *a*)-specific production rates of water-extractable polysaccharides were significantly higher for "in-patch" than for "out-patch" samples (0.5 vs. 0.3 μg C [μg Chl *a*]$^{-1}$ h^{-1}, respectively). Together with the higher photochemical efficiency of photosystem II (F_v/F_m), this indicates enhanced photosynthetic performance in response to iron fertilization. In addition, the nocturnal polysaccharide consumption rates were also enhanced by iron release, causing a striking increase in the diel dynamics of polysaccharide concentration. An iron-stimulated increase in diel dynamics was also observed in the fluorescence and size of pico- and nanophytoplankton cells (measured by flow cytometry) and is indicative of enhanced phytoplankton growth. Diurnal polysaccharide production by phytoplankton inside the patch was light-limited when they were incubated at intensities below ca. 200 μmol m^{-2} s^{-1} (daytime average). These irradiance levels correspond to those at 20- to 30-m depth in situ, whereas the upper mixed layer was frequently several-fold deeper due to storms. Therefore, these first measurements of phytoplankton

* Corresponding author. Tel.: +31 50 3636140; fax: +31 50 3632261.
E-mail address: t.van.oijen@biol.rug.nl (T. van Oijen).

0304-4203/$ - see front matter
doi:10.1016/j.marchem.2004.06.039

carbohydrates during an in situ iron release experiment have revealed that both light and iron availability are the key factors controlling the synthesis of storage carbohydrates in phytoplankton and, hence, the development of diatom blooms in the Southern Ocean.

Keywords: Algae; Iron fertilization; Light; Carbohydrates; Photosynthesis; Southern Ocean

1. Introduction

A large part of the Southern Ocean is characterized by low phytoplankton biomass throughout the year even though major nutrients are in ample supply. Results of shipboard iron enrichment mesocosm studies suggested that phytoplankton productivity is limited by the low iron availability (De Baar et al., 1990; Martin et al., 1990; Buma et al., 1991; Van Leeuwe et al., 1997). This was further supported by a mesoscale in situ fertilization approach, which had previously been taken in another high-nitrogen low-chlorophyll (HNLC) region, namely, the equatorial Pacific Ocean (Martin et al., 1994; Coale et al., 1996).

The first in situ iron release experiment in the Southern Ocean—Southern Ocean Iron RElease Experiment (SOIREE)—has been conducted in late austral summer 1999 in the Pacific sector (Boyd et al., 2000) and caused elevated algal photosynthetic competence (Boyd and Abraham, 2001), chlorophyll *a* (Chl *a*) concentrations and primary productivity (Gall et al., 2001b). The iron addition led to a shift in species composition towards larger diatom species (i.e., *Fragilariopsis kerguelensis*) (Gall et al., 2001a). Due to high temporal variations in physical conditions, such as day-length, cloudiness and the vertical stability of the water column, the results of SOIREE cannot be readily extrapolated to other seasons. The second in situ fertilization experiment—EisenEx/CARbon dioxide Uptake by the Southern Ocean (CARUSO)—was performed in the austral spring (November 2000) with the overarching goal to investigate if the absence of diatom spring blooms in large parts of the Southern Ocean was due to iron limitation (Gervais et al., 2002). During this experiment, we studied the effects of iron availability and irradiance on storage carbohydrate production by phytoplankton.

Carbohydrates are a key structural component of cell membranes and serve as a storage reserve. In diatoms, the storage carbohydrate is β-1,3-glucan, which can be isolated by hot-water extraction (Hama and Handa, 1992). Because they facilitate continued growth in darkness by providing energy and carbon skeletons for protein synthesis, storage carbohydrates are important for phytoplankton growth in a dynamic light environment (Cuhel et al., 1984; Granum and Myklestad, 2001). In a light–dark cycle, healthy diatom cultures show strong diel dynamics in the storage carbohydrate pool, with high production during the light period and subsequent consumption in the dark (Hitchcock, 1980).

The production of carbohydrates by phytoplankton in the Southern Ocean could be controlled by iron and light availability. Iron is an essential element of components that play a role in photosynthesis, respiration and nutrient assimilation processes (Geider and La Roche, 1994). Laboratory experiments have provided evidence that the primary target of iron limitation in phytoplankton is the photosynthetic machinery. The paucity of iron decreases the quantum yield of photosynthesis and light absorption due to a decrease in cellular pigment content (Van Leeuwe and De Baar, 2000; Milligan and Harrison, 2000; Davey and Geider, 2001). Storage carbohydrates are synthesized from first products of the Calvin–Benson Cycle (Salisbury and Ross, 1992), which is driven by energy supplied by the photosynthetic reactions. Hence, synthesis of storage carbohydrates should be also suppressed by iron limitation.

Photosynthesis and thus carbohydrate production rely on light availability. The open ocean zone of the Southern Ocean is characterized by deep vertical mixing induced by strong winds. The vertically mixed layer can exceed 100 m and thus the depth of the euphotic zone. Phytoplankton in this layer are exposed to low average irradiance and are subject to a highly dynamic light environment with alternating periods of high (near-surface) and low (at depth) light. Model calculations suggest that the light climate may

set the upper limits of phytoplankton biomass in the Southern Ocean (Mitchell et al., 1991; Nelson and Smith, 1991). However, these models are incomplete because they do not yet include iron supply as a steering factor. SWAMCO, an ecological model that does include iron, suggests a dual role for iron and light in driving the magnitude of a diatom bloom in the Southern Ocean (Lancelot et al., 2000).

We hypothesize that the amount of water-extractable carbohydrates in the particulate fraction will increase after iron fertilization, specifically in the large-size fraction, in correlation with an increase in biomass and a floristic shift towards large phytoplankton species. This hypothesis was tested by in situ measurements of carbohydrates in <10 and >10 μm phytoplankton inside and outside the iron-fertilized patch. Further, we hypothesize that the diurnal production and nocturnal consumption of water-extractable carbohydrates by phytoplankton cells will increase in response to iron addition. This was tested by 24-h deck incubations with "in-patch" and "out-patch" samples. Finally, we investigate whether carbohydrate production is limited by light availability. We tested the hypothesis that the production inside the patch is light-limited by performing 24-h deck incubations with in-patch samples at three different light intensities. During the deck incubations, in addition to carbohydrates, fluorescence and size of some pico- and nanophytoplankton cells (measured by flow cytometry) and several photosynthetic parameters [fast repetition rate (FRR) fluorometry] were studied.

2. Materials and methods

2.1. General description

An iron release experiment was performed in the Atlantic Sector of the Southern Ocean (~21°E, ~48°S) in austral spring (6–29 November 2000) during the cruise ANT XVIII/2 of RV Polarstern. In 7 November (t=0), a solution of acidified iron sulphate containing the inert tracer SF_6 was released over an area of around 50 km^2 close to the centre of an eddy. This eddy likely originated from the Antarctic Polar Front and had been identified by inspection of current velocities and directions (Strass et al., 2001). In 15 and 24 November, two additional iron releases were conducted without the addition of SF_6. Horizontal surveys of SF_6 concentration, major nutrient concentrations and of concentrations of various chemical forms of iron were conducted throughout the experiment (Watson et al., 2001; Croot et al., 2001). The downwelling photosynthetically available radiation (E_a; PAR, 400–700 nm) was measured every minute with a LI-COR 192SA cosine quantum sensor.

2.2. In situ measurements

In situ measurements were performed both inside and outside the Fe-enriched water body ("the patch") throughout the experiment. "In-stations" were situated at the highest SF_6 concentrations observed, whereas "out-stations" were within the waters of the eddy that showed background SF_6 concentrations (Watson et al., 2001). Samples were collected by a rosette sampler (Sea-Bird SBE 32) equipped with 24 bottles (12 l each), conductivity–temperature–depth (CTD) probes (Sea-Bird Electronics 911 plus) and a Haardt fluorometer. The carbohydrate concentration was measured in samples from 10-, 20-, 40-, 60-, 80- and 100-m depth.

2.3. Deck incubations

Table 1 provides an overview of all deck incubation experiments performed during the cruise. The experiments were carried out under trace metal clean conditions with natural phytoplankton populations that were kept at ambient temperature using running surface seawater. Two types of experiments were performed. During the first type (A), phytoplankton was sampled inside and outside the patch with a trace metal clean inlet (the "torpedo") that was towed alongside the research vessel at a distance of several meters from the hull. Sample locations were again selected based on SF_6 concentrations. Samples were incubated for 24 h in 4 l polycarbonate bottles in a deck incubator at 60% of the ambient light intensity. During the second type of experiments (B), 24-h incubations were carried out at 60%, 30% and 10% of the ambient light intensity with phytoplankton that was sampled inside the patch with either the torpedo or the rosette sampler.

Table 1
Summary of the deck incubation experiments performed during ANT 18/2

Date	Daynr[a]	Daily PAR (mol^{-2} day^{-1})	Sample location[b]	Chl *a* ($\mu g\ l^{-1}$)		NO_3 ($\mu mol\ L^{-1}$)	Si ($\mu mol\ L^{-1}$)	PO_4 ($\mu mol\ L^{-1}$)	Fe ($nmol\ L^{-1}$)
				>0.8 μm	>10 μm				
Type A									
14 November 2000	6	26.3	Out	0.45	n.d.	22.80	12.06	1.58	0.46
			In	0.85	n.d.	23.02	14.44	1.59	4.39
18 November 2000	10	14.0	Out	0.46	0.15	22.84	12.25	1.57	0.74
			In	1.00	0.37	22.85	13.93	1.60	2.60
27 November 2000	19	54.8	Out	0.61	0.28	22.34	10.74	1.50	0.41
			In	2.08	1.18	21.56	10.46	1.47	0.78
Type B									
11 November 2000	3	46.2	In	0.61	n.d.	23.19	14.52	1.67	4.69
16 November 2000	8	48.4	In	0.91	0.28	23.06	13.80	1.61	3.44
20 November 2000	12	35.9	In	1.61	n.d.	21.26	12.76	1.08	2.79
24 November 2000	16	44.4	In	1.60	n.d.	21.98	12.14	1.53	2.37

[a] Daynr is the number of days since the first Fe release. n.d. is 'not determined'.
[b] Sample location is either outside ('out') or inside ('in') the Fe-fertilized patch.

Experiment A was carried out three times and experiment B four times during the Fe-fertilization experiment. Before the start of an experiment, samples were taken for concentrations of major nutrients, Fe concentration and Chl *a* concentration. Samples for flow cytometry and carbohydrate analysis were taken from the incubation flasks at dawn, dusk and the next morning. At dusk, samples were also taken for fast repetition rate fluorometry.

2.4. Analysis methods

2.4.1. Major nutrient concentration analysis

The concentrations of nitrate, phosphate and silicate were determined on board using a Technicon II Autoanalyzer following standard methods.

2.4.2. Iron concentration analysis

All samples for iron analysis were collected in 125-ml polyethylene bottles, and were buffered at pH 3.2 with 10 mol L^{-1} formic acid—2.4 mol L^{-1} ammonium formate buffer solution. The determined Fe is a chemically labile species, which is in unfiltered seawater and strongly reacts with 8-hydroxyquinoline resin at pH 3.2. The sample pretreatment was performed in a laminar flow clean air hood located in the on-board container laboratory. Concentrations of Fe(III) in the buffered samples were determined with an automatic Fe(III) analyzer (Kimoto Electric) using chelating resin concentration and chemiluminescence detection (Obata et al., 1993, 1997).

2.4.3. Chl a analysis

Immediately after sampling, 1000 ml samples were filtered on a Whatman GF/F filter. The filters were ground in 10 ml 90% acetone, extracted at 4 °C for 2 h, and centrifuged. The extract fluorescence was measured with a Turner Design Model 10-AU digital fluorometer before and after acidification to 0.003 N HCl. The Chl *a* concentration was calculated according to Arar and Collins (1992).

2.4.4. Carbohydrate analysis

Aliquots of 1–4 L were filtered on pre-combusted (350 °C) 50 mm GF/F Whatman filters (total fraction) and 10 μm polycarbonate membranes under gentle vacuum pressure (<200 mm Hg). The filters were stored at −20 °C until analysis. They were extracted in water (Milli-Q) in sealed glass test tubes placed in a water bath for 1 h at 80 °C. Afterwards, the tubes were cooled and centrifuged for 5 min at 715 g. The monosaccharide and polysaccharide concentration in the extract were determined for three replicates with the colorimetric 2,4,6-tripyridyl-s-triazine (TPTZ)-method described by Myklestad et al. (1997), with minor modifications. D(+)-Glucose was used as the standard and measurements were corrected for blank filters. The coefficient of

variation of replicates was ~1%. Depth profiles of carbohydrate concentrations at the stations were based on single samples at each depth. Before the iron-release experiment, five times duplicate seawater samples were taken to test the reliability of the method for field samples. The coefficient of variation varied between 1% and 7%.

For samples of the last eight stations that were visited, the concentration of the non-water-extractable fraction of the carbohydrates that remained on the filter was also determined. These carbohydrates, which are mainly structural components of the cell wall, were hydrolyzed with concentrated sulphuric acid (97 wt.%). The phenol-sulphuric acid method (Dubois et al., 1956) was used to determine the carbohydrate concentration. Again, D(+)-Glucose was used as the standard. Because different monosaccharides have been found to yield different absorbances in equimolar solutions using this method, it is more semi-quantitative than quantitative.

The carbohydrate concentration is indicated in μg Glucose (Glc)-equivalents L^{-1}, unless indicated otherwise. In case the concentration is presented in μg C L^{-1}, the conversion from carbohydrate to carbon concentration was based on the elemental composition of glucose (40 wt.% is C), arguably the most abundant molecule in water-extractable microalgal polysaccharides (Hama and Handa, 1992).

2.4.5. Polysaccharide production vs. irradiance curves

Based on the diurnal production of carbohydrates, measured at three light intensities during the type B experiments, polysaccharide production–irradiance curves were constructed. To this end, the average production rate of polysaccharides was plotted against the average PAR received during the light period for each of the three light treatments. The data were fitted using an exponential function identical to the one of Webb et al. (1974):

$$P = P_m^* \left[1 - \exp\left(- \alpha^* \frac{E}{P_m^*} \right) \right]$$

where, in this case, P_m^* is the maximum carbohydrate production rate normalized to Chl *a* in μg C [μg Chl *a*]$^{-1}$ h^{-1}, E is the irradiance (PAR) in μmol photons m^{-2} s^{-1} and α^* is the initial slope of the curve in μg C [μg Chl *a*]$^{-1}$ h^{-1} (μmol photons m^{-2} s^{-1})$^{-1}$. The light saturation parameter E_k[PAR] in μmol photons m^{-2} s^{-1} was calculated as P_m^*/α^*. In this model, neither photoinhibition at high irradiance nor the possible consumption of carbohydrates were taken into account.

2.4.6. Fast repetition rate (FRR) fluorometry

The photosynthetic status of phytoplankton was assessed by using the custom-built FRR fluorometer (Kolber et al., 1998). The instrument records a suite of photosynthetic parameters, including the minimal, maximal and variable fluorescence yield (F_0, F_m and F_v), the potential photochemical efficiency of photosystem II (F_v/F_m), the functional absorption cross section of photosytem II (σPSII), the time constant (i.e., the reciprocal rate) for re-oxidation of the first quinone acceptor of PSII, Q_a, (t-Q_a), and the time constant for re-oxidation of the plastoquinone pool (t-PQ). t-Q_a characterizes the rate of electron transport on the acceptor side of PSII, whereas t-PQ does the rate of electron transport between PSII and PSI (see, for detail, Kolber et al. (1998)). Samples were kept on ice in the darkness for at least 1 h before FRR measurements.

2.4.7. Flow cytometry

Samples were taken in plastic 20-ml bottles that were kept on melting ice and in the dark until analysis. They were analyzed 1 to 4 h after sampling. Samples were counted with a bench top flow cytometer (Coulter XL-MCL) equipped with a 15-mW laser. The excitation wavelength was 488 nm. Two emission bands were distinguished, in the orange (PE) and red (chlor.) region of the light spectrum: FL2 (575±20 nm) and FL3 (>630 nm), respectively. The low ambient temperature (2–5 °C) prohibited long exposure of the live samples to room temperature. Therefore, the measuring time was limited to 5 min. At least 5000 cells were counted. Based on their fluorescence emission and scatter characteristics, three distinguishable clusters of cells could be assigned. These included *Synechococcus* cells (distinguished based on the PE fluorescence), a ca. 1 μm large picoeukaryote and a group with a mixture of small eukaryotes (ca. 2–5 μm). For each of these clusters, the forward light scatter (a measure of cell size) and the fluorescence

(a measure of pigmentation) were determined. Large phytoplankton cells (>5–10 μm) could not be analyzed quantitatively and were excluded from the analysis.

2.5. Statistical analysis

Multi-factor analyses of variance (ANOVA) were performed for the various parameters measured during the deck incubations, following the procedure described by Underwood (1997). Significant factors were identified with *F*-tests. Factors tested included time (number of days since first iron release), sample location (inside or outside patch) and, if applicable, time of sampling (AM/PM). Tukey post hoc tests were used to determine which means were significantly different from which others at a 95% confidence level. The regression coefficient of the fit of the polysaccharide production–irradiance curves was determined using Sigmaplot 8.0.

3. Results

3.1. In situ measurements

In the centre of the patch, the near-surface (10-m depth) concentration of the water-extractable carbohydrates of the particulate fraction (hereafter "water-extractable carbohydrates" for brevity) increased during the experiment from 21 to 32 μg L^{-1} (Fig. 1A). The areal amount (the integral over 0- to 100-m depths) almost doubled from 1375 to 2289 mg m^{-2}. Outside the patch, the near-surface concentration remained constrained in the range between 15 and 22 μg L^{-1} (Fig. 1B), the areal amount between 1089 and 1480 mg m^{-2}.

Generally, the water-extractable carbohydrate concentration decreased with depth (Fig. 1). A more uniform distribution of carbohydrates over the euphotic zone was observed after three intense storms, which were encountered on days 5, 13 and 19 following the first iron release. For example, after the first storm, carbohydrate concentrations of ca. 27 μg L^{-1} were recorded over the range of depths from 0 to 60 m. In contrast, on day 12, after a period of calm weather and strong stratification, the concentration was maximal near the surface (39 μg L^{-1}) and steeply decreased to 9.2 μg L^{-1} at 60-m depth.

During the first week after the Fe release, the areal amount of water-extractable carbohydrates in both <10 μm and >10 μm phytoplankton increased by ~50% (Fig. 2A). In the second week, the amount of carbohydrates in <10 μm phytoplankton remained constant whereas the amount in >10 μm phytoplankton decreased to approximately the initial level. Over the final 5 days of the experiment, inside the patch, the areal amount in the latter size fraction sharply increased from 595 to 1419 mg m^{-2}, whereas the amount in <10 μm phytoplankton decreased from 1086 to 870 mg m^{-2}. As a result, at the end of the experiment, the contribution of water-extractable carbohydrates in >10 μm phytoplankton to the total amount of water-extractable carbohydrates had increased from the initial 37% to 62%. For both size fractions, the areal amount of water-extractable carbohydrates was relatively constant outside the patch.

The entire pool of water-extractable carbohydrates can be divided into a pool of monosaccharides and a pool of polysaccharides. The ratio of polysaccharides to monosaccharides (weight/weight) in <10 and >10 μm phytoplankton varied between 1.3–2.3 and 0.4–0.9, respectively. The relative contributions of the two size classes to the two pools showed only minor variations with depth (not shown). The areal amount of monosaccharides (0–100 m) inside the patch varied between 640 and 840 mg m^{-2} over the first 2 weeks of the experiment. During this period, monosaccharides were distributed evenly between <10 and >10 μm phytoplankton (Fig. 2B). Over the last week, the amount of monosaccharides in <10 μm phytoplankton decreased from 396 to 266 mg m^{-2}. The amount of monosaccharides in >10 μm phytoplankton increased from 414 to 796 mg m^{-2}, which corresponded to 75% of the total amount of monosaccharides. The amount of monosaccharides was lower outside than inside the patch and varied between 200 and 400 mg m^{-2} for both size fractions.

In the first 2 weeks, the areal amount of polysaccharides (0–100 m) in <10 μm phytoplankton was two to four times higher than in >10 μm phytoplankton, both outside and inside the patch

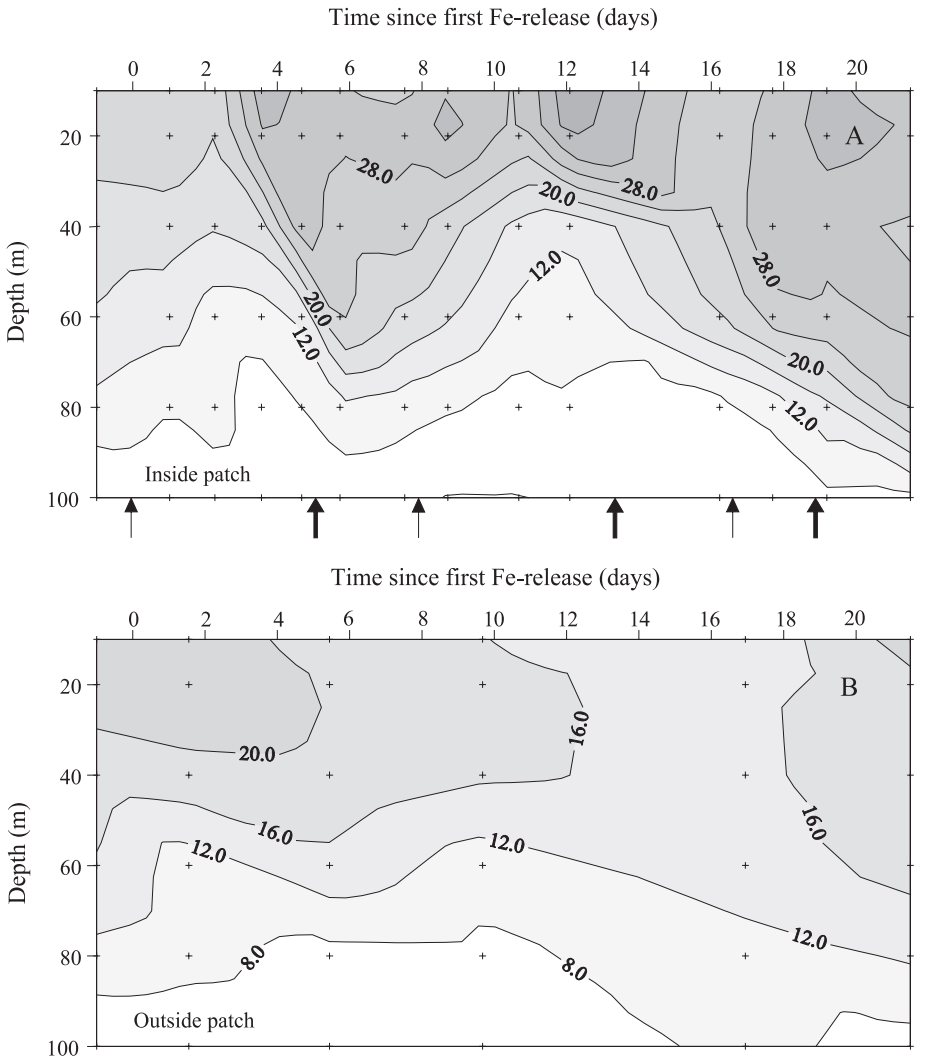

Fig. 1. Temporal evolution of the total water-extractable carbohydrate concentration in the particulate fraction (in μg Glc-equiv. L^{-1}) in the upper 100 m of the water column, inside (A) and outside (B) the Fe-enriched water body during the fertilization experiment. The contours are based on linear interpolation of the data (crosses). The arrows at the bottom of panel A mark the times of the three iron infusions (thin arrows) and of the three major storms (thick arrows).

(Fig. 2C). During the last week, the amount of polysaccharides in >10 μm phytoplankton increased from 178 to 623 mg m^{-2} inside the patch and became higher than in <10 μm phytoplankton. For the greater part of the experiment, the amount of polysaccharides was higher inside than outside the patch.

We compared the carbohydrate data to Chl *a* data collected at the same stations (Chl *a* data courtesy of U. Riebesell and others; see also Gervais et al., 2002). The ratio of the water-extractable carbohydrates to Chl *a* decreased with depth from 31.3±12.2 at 10 m to 17.3±5.6 at 100 m (weight/weight, average and standard deviations of all 20 stations). The decrease was more pronounced in the ratio of polysaccharides to Chl *a* (17.1–8.4) than in the ratio of monosaccharides to Chl *a* (14.2–8.9). During the course of the experiment, inside the patch, there was a decline in the ratio of the areal amount (0–100 m) of water-extractable carbohy-

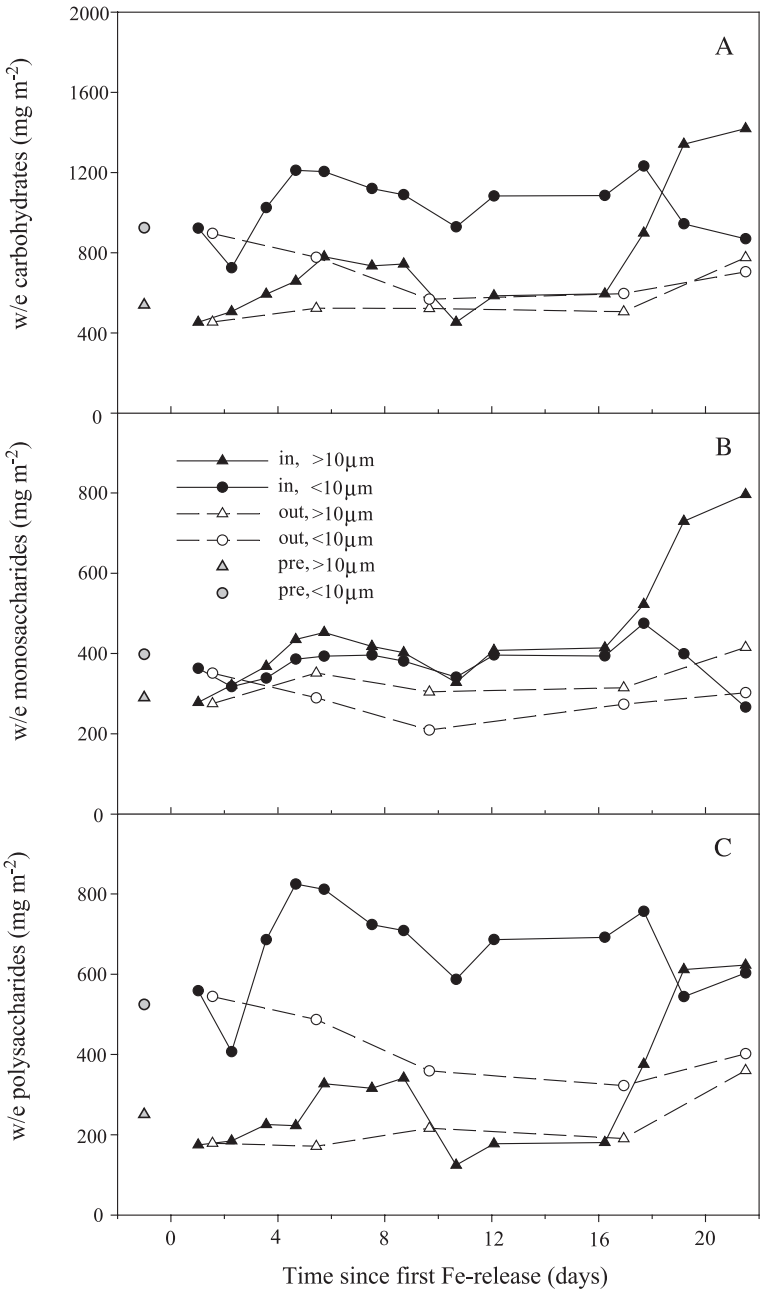

Fig. 2. Temporal evolution of the areal amount (Glc-equiv., integral between 0- and 100-m depth) of (A) the total water-extractable (w/e) carbohydrates, (B) the monosaccharides and (C) polysaccharides in <10 μm phytoplankton and >10 μm phytoplankton inside and outside the Fe-enriched patch during the experiment. Symbols are explained in the legend in panel B. Note the difference in the scale of the *y*-axis between the panels.

drates to that of Chl *a* from 32 to 11 (w/w) (Fig. 3). Outside the patch, there also appeared to be a negative trend in this ratio.

For eight stations, the concentration of structural, non-water-extractable carbohydrates was also measured, which allowed for the contribution of water-ex-

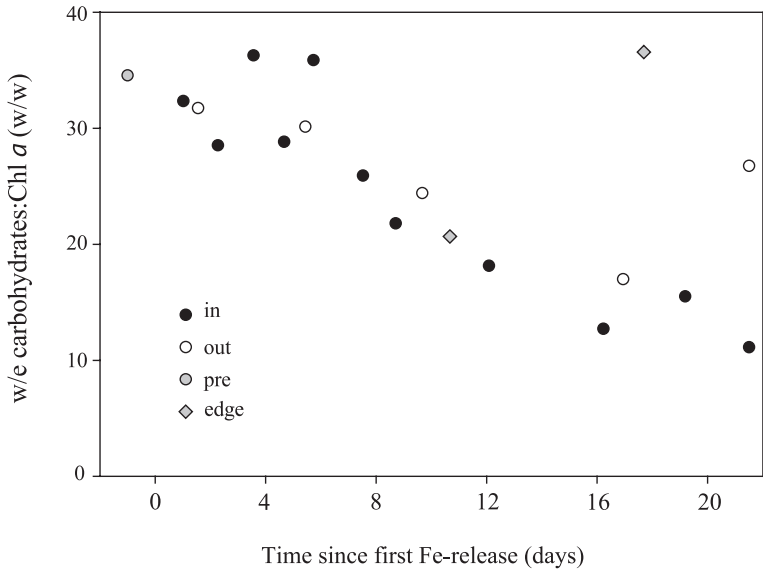

Fig. 3. Changes over time in the ratio of the amount (Glc-equiv.) of water-extractable carbohydrates to Chl *a* (integrals between 0- and 100-m depth) inside and outside the Fe-fertilized patch over the course of the experiment. Grey diamonds are data points for which Chl *a* samples were likely taken at the edge of the patch, based on the SF_6 values. The grey circle is the value before iron addition. Chl *a* data are taken from Gervais et al. (2002).

tractable carbohydrates to the total carbohydrate pool to be determined (Fig. 4). This contribution was 73±5% at 10 m and decreased to 50±7% at 100-m depth.

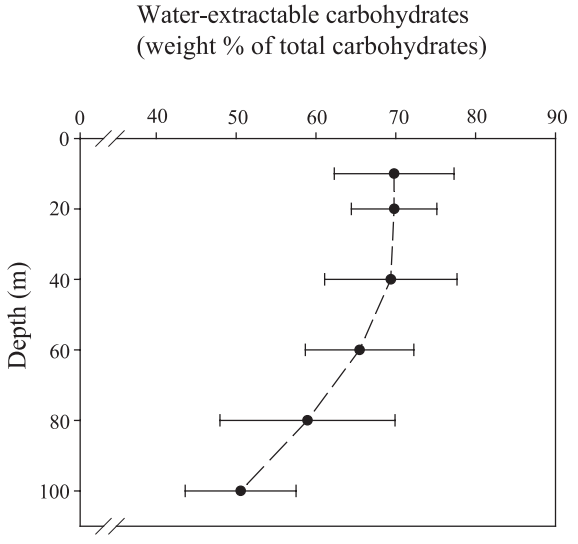

Fig. 4. The relative contribution of water-extractable carbohydrates to the total carbohydrate pool in the upper 100 m of the water column. Error bars indicate standard deviation (n=8).

4. Deck incubation experiments

4.1. Type A

Deck incubations of type A were carried out on days 6, 10 and 19 after the first Fe release (Table 1). The light conditions varied between the incubations—from very cloudy skies and low PAR on day 10 to almost cloudless skies and high PAR on day 19 (Table 1). Iron concentrations varied between 0.78 and 4.7 nmol L^{-1} and between 0.41 and 0.74 nmol L^{-1} in in-patch and out-patch bottles, respectively. Concentrations of major nutrients NO_3, Si and PO_4 were high in all bottles (Table 1).

The Chl *a* concentration in in-patch samples increased from 0.85 μg L^{-1} on day 6 to 2.08 μg L^{-1} on day 19, whereas that in out-patch samples was roughly constant (0.45–0.61 μg L^{-1}) (Table 1). The contribution of large phytoplankton (>10 μm) to the total Chl *a* in in-patch samples increased from 37% on day 10 to 57% on day 19. In out-patch samples, this contribution increased to a lesser extent, from 32% to 46%. These patterns are consistent with the size-fractionated Chl *a* analysis of Gervais et al. (2002).

The increase in Chl *a* concentration in in-patch bottles was accompanied by an increase in the variable fluorescence, F_v (Table 2), which is a good proxy of Chl *a* concentration (Gorbunov, unpublished data). F_v and the maximal quantum yield of photochemistry in PSII (F_v/F_m) were both significantly higher in in-patch bottles than in out-patch ones (ANOVAs, see Table 2; Tukey post hoc tests). The ratio F_v/F_m was, on average, 0.5 in in-patch bottles vs. 0.4 in out-patch bottles. The functional absorption cross section of photosystem II (σPSII) was significantly lower in in-patch bottles than in out-patch bottles (Table 2). The re-oxidation rates of Q_a (t-Q_a) were also significantly lower in in-patch bottles; the re-oxidation rates of the plastoquinone pool (t-PQ) were undistinguishable between in- and out-patch bottles (Table 2).

Flow cytometric analysis revealed that the average number of phytoplankton cells was 13,800±2600 cells ml^{-1} (cells>5–10 μm are excluded by the method). On average, 14±3% were *Synechococcus* cells, 59±6% pico-eukaryotes and 27±4% small eukaryotes. There were no significant differences in cell numbers and composition between the treatments and experiments.

The average chlorophyll fluorescence and cell size increased during the day and decreased at night (Fig. 5A–C). Both parameters were significantly dependent on sample location (ANOVAs—size: n=30, F=52.3, p<0.001; fluorescence: n=30, F=63.6, p<0.001) and significantly higher in the in-patch samples (Tukey post hoc test). The diurnal increase in size was also significantly higher for cells from inside the patch (ANOVA: n=11, F=37.2, p<0.001; Tukey post hoc test); their increase was highest on day 19, the day with the highest light intensity (Fig. 5C). The clusters of both picoeukaryotes (Fig. 5G–I) and small eukaryotes (Fig. 5J–L) showed qualitatively similar patterns, with the average fluorescence and size being 5–10 times higher for the latter cluster. However, *Synechococcus* cells (Fig. 5D–F) did not show any difference in either cell size or fluorescence between in- and out-patch samples and between morning or afternoon.

Like the cell size, the concentration of water-extractable carbohydrates of the particulate fraction exhibited clear diel patterns in all three experiments (Fig. 6A–C). These patterns were more pronounced in the polysaccharide fraction (Fig. 6G–I) than in the monosaccharide fraction (Fig. 6D–F). The polysaccharide concentration was significantly higher in the in-patch bottles (ANOVA: n=36, F=78.2, p<0.001; Tukey post hoc test). The Chl *a*-normalized rates of net diurnal polysaccharide production were also significantly higher in in-patch bottles (ANOVA, see Table 2; Tukey post hoc test). For the in-patch bottles, the polysaccharide production rate was highest on day 19: 0.68 μg C [μg Chl *a*]$^{-1}$ h^{-1}. On average, the polysaccharide concentration increased by 364% and was over 100 μg L^{-1} at the end of the light period, which was threefold higher than the maximum concentration observed in situ (Figs. 1 and 6A–C).

For the experiments on days 10 and 19, data on the carbohydrate concentration in the >10 μm phytoplankton fraction were collected. Also for this fraction, the polysaccharide concentration was significantly higher in in-patch bottles (ANOVA: n=20,

Table 2
Photosynthetic parameters measured by FRR fluorometry and diurnal carbohydrate production rates during deck incubations of type A (see Materials and methods and Table 1)

	Day 6		Day 10		Day 19		ANOVA[a]	
	Out	In	Out	In	Out	In	*F*-ratio	*p*-value
F_v	1204 (257)	2026 (160)	1947 (334)	3763 (205)	1388 (29)	7143 (480)	295.4	<0.001
F_v/F_m	0.42 (0.02)	0.48 (0.01)	0.40 (0.05)	0.50 (0.01)	0.38 (0.02)	0.50 (0.01)	45.2	0.001
σPSII ($Å^2$/quanta)	389 (22)	372 (39)	438 (2)	361 (1)	439 (34)	368 (13)	16.5	0.007
t-Q_a (μs)	1039 (7)	802 (127)	1253 (12)	649 (215)	1173 (–)	866 (89)	26.7	0.004
t-PQ (μs)	4608 (206)	4762 (726)	5460 (438)	5213 (64)	4741 (1076)	4426 (392)	0.2	0.703
CHO prod[b]	0.34 (0.04)	0.32 (0.04)	0.33 (0.08)	0.47 (0.01)	0.17 (0.00)	0.68 (0.02)	74.4	<0.001

Data in parenthesis are standard deviations.
[a] The *F*-ratio and *p*-value listed are of ANOVAs for the factor "sample location".
[b] Water-extractable polysaccharide production rate (μg C [μg Chl *a*]$^{-1}$ h^{-1}).

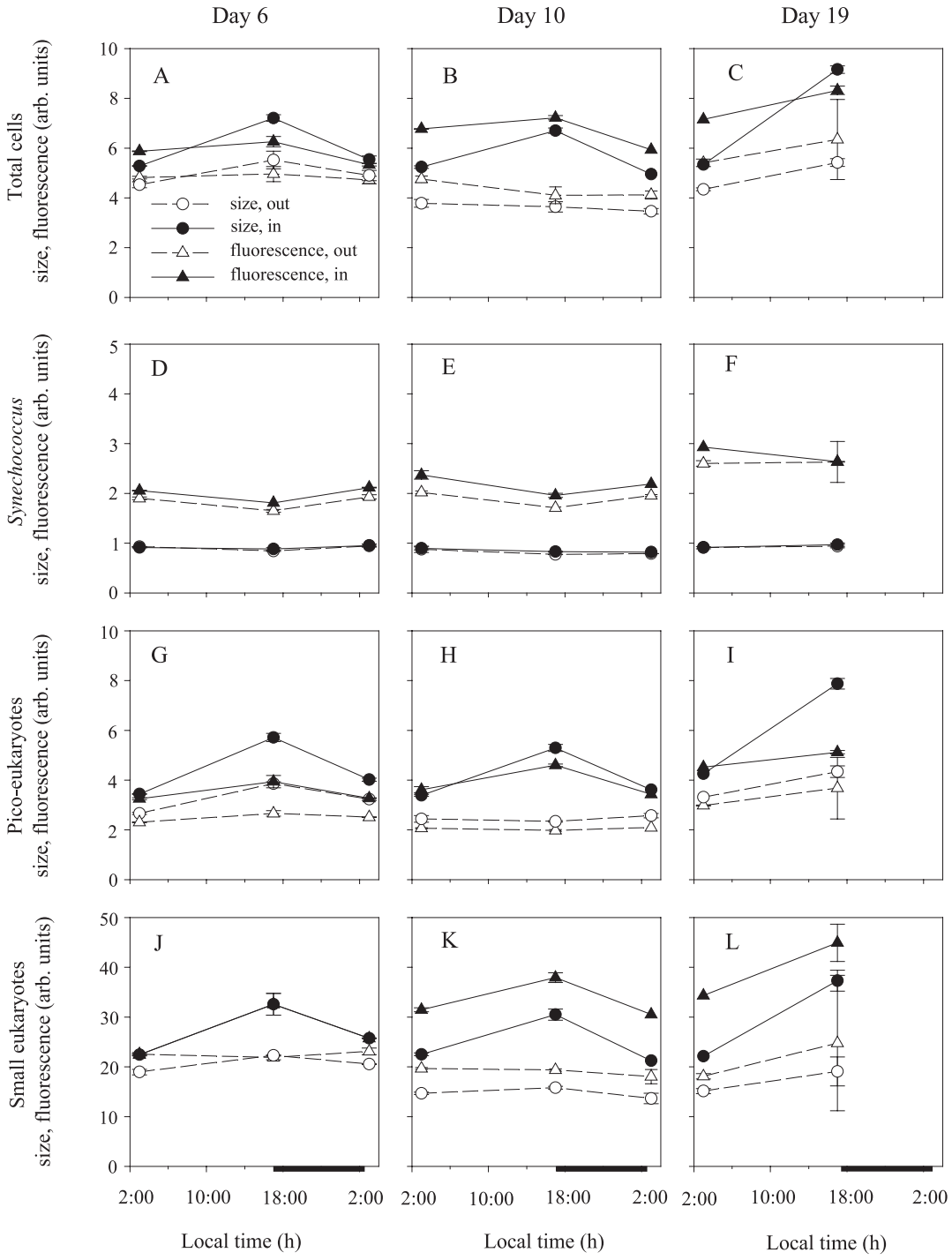

Fig. 5. Diel changes in cell size and cell fluorescence for (A–C) the whole phytoplankton community, (D–F) *Synechococcus*, (G–I) pico-eukaryotes and (J–L) small eukaryotes during deck incubations with samples from inside and outside the Fe-enriched patch. These incubations were performed (A, D, G, J) 6 days, (B, E, H, K) 10 days and (C, F, I, L) 19 days after the first Fe release. Error bars indicate standard deviations (n=2). Black bars indicate the dark period. Symbols are explained in the legend in panel A.

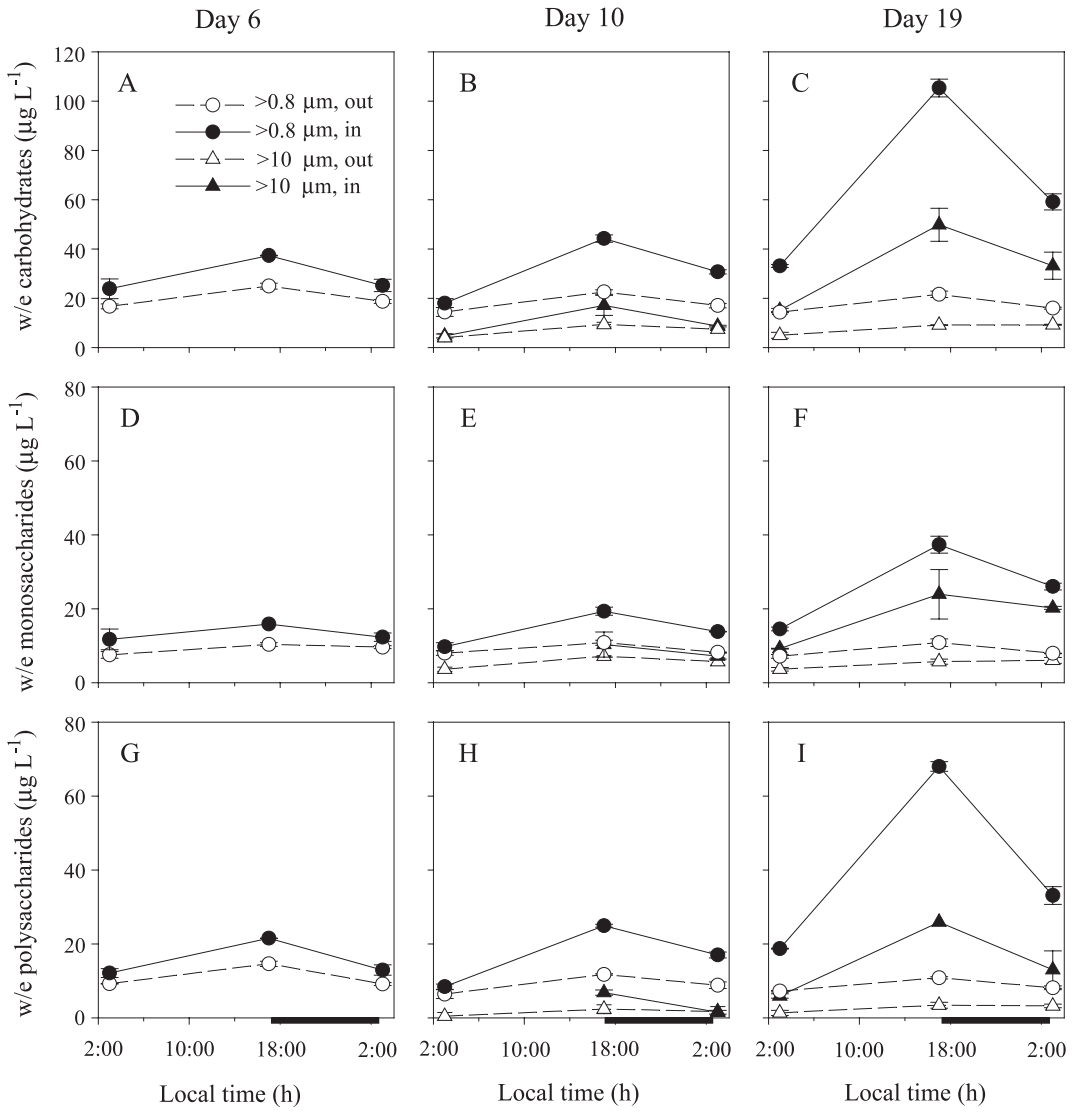

Fig. 6. Diel changes in the amount (Glc-equiv.) of (A–C) the total water-extractable carbohydrate pool, (D–F) the monosaccharide fraction and (G–I) the polysaccharide fraction in total (>0.8 μm) and micro- (>10 μm) phytoplankton during 24 h deck incubations at 60% of the ambient light intensity with samples from inside and outside the Fe-enriched patch. The incubations were performed (A, D, G) 6 days, (B, E, H) 10 days and (C, F, I) 19 days after the first Fe release. Error bars indicate standard deviations (n=2). Black bars indicate the dark period. Symbols are explained in the legend in panel A.

F=33.8, p<0.001; Tukey post hoc test). The relative contribution of polysaccharides in the >10 μm phytoplankton fraction to the total polysaccharide pool was higher in in-patch samples, 27% vs. 20% on day 10 and 38% vs. 31% on day 19 (afternoon values). On day 19, the net polysaccharide production rate of the >10 μm phytoplankton was 0.21 in out-patch samples and 0.48 μg C [μg Chl a]$^{-1}$ h^{-1} in in-patch samples.

4.2. Type B

Deck incubations of type B were carried out with in-patch samples at 3, 8, 12 and 16 days after

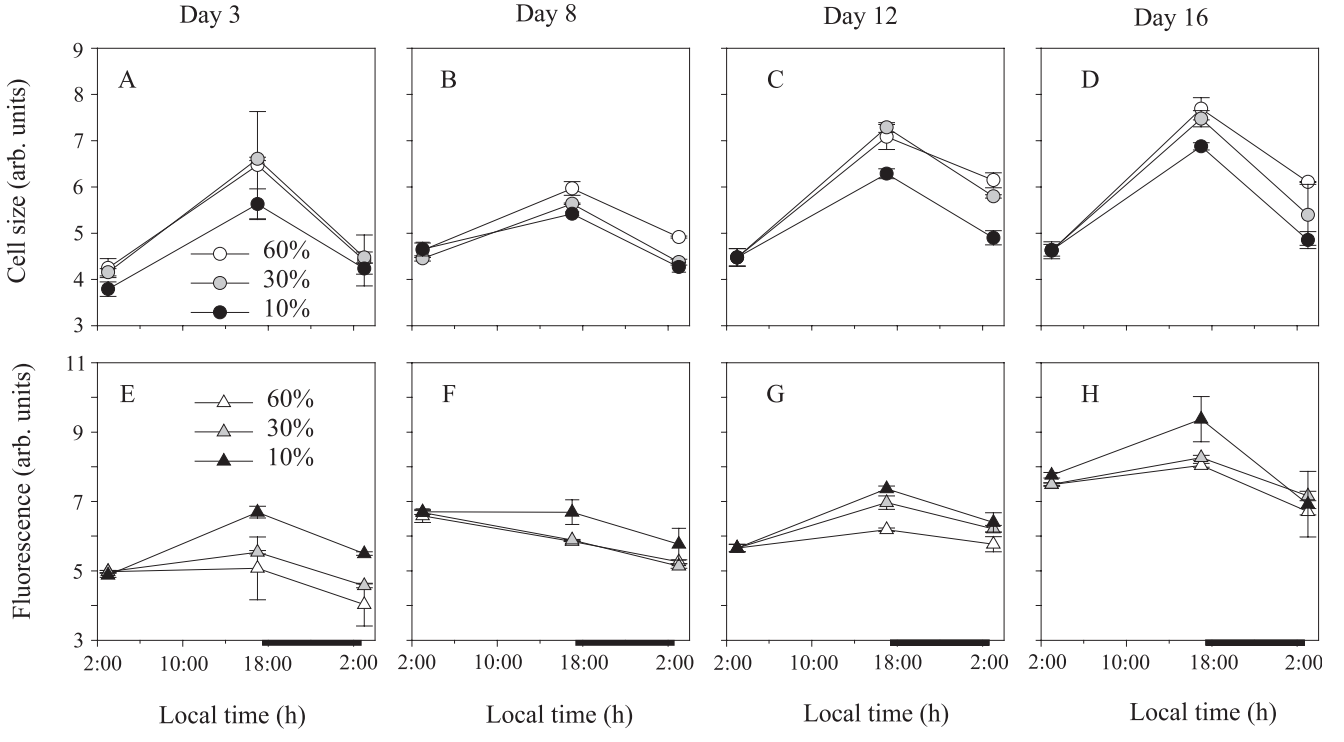

Fig. 7. Changes in cell size and cell fluorescence for all cells analyzed with flow cytometry during deck incubations of samples from inside the Fe-enriched water body at 10%, 30% and 60% of the ambient light intensity performed (A, E) 3 days, (B, F) 8 days, (C, G) 12 days, and (D, H) 16 days after the first Fe release. Error bars indicate standard deviations (n=2). Black bars indicate dark period. Symbols are explained in the legends in panels A and E.

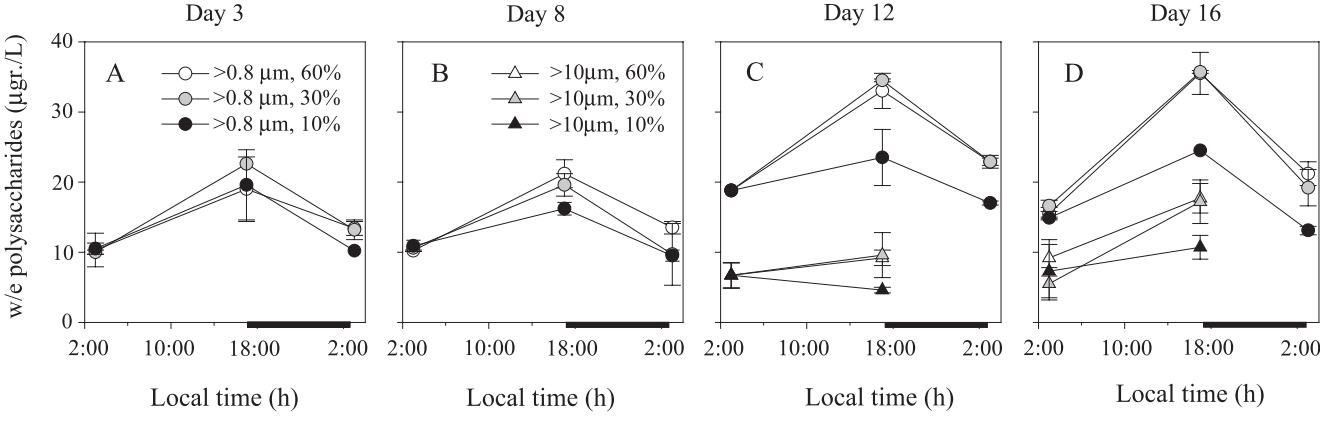

Fig. 8. Diel changes in the amount (Glc-equiv.) of water-extractable polysaccharides for total phytoplankton (>0.8 µm) and >10 µm phytoplankton during 24 h deck incubations at 10%, 30% and 60% of the ambient light intensity with samples from inside the Fe-enriched patch. These incubations were performed (A) 3 days, (B) 8 days, (C) 12 days and (D) 16 days after the first Fe release. Error bars indicate standard deviations (n=2). Black bars indicate dark period. Symbols are explained in the legends in panels A and B.

the first iron release. Light conditions were similar between the experiments, the daily PAR irradiance varied between 36 and 48 mol photons m^{-2} day^{-1} (Table 1). The Fe concentrations were high in all incubations, between 2.4 and 4.7 nmol L^{-1} (Table 1) and major nutrient concentrations were also high.

The Chl *a* concentration increased from 0.6 μg L^{-1} on day 3 to 1.6 μg L^{-1} on day 16. This increase was accompanied by an increase in F_v from 1792 to 5282. The F_v/F_m varied between 0.41 and 0.52 and was significantly higher for cells incubated at 10% of the ambient light compared to at 60% (ANOVA: n=12, F=10.7, p=0.01; Tukey post hoc test).

The average cell volume and chlorophyll fluorescence exhibited clear diel variations at all three light intensities (Fig. 7). The diurnal increase in cell size and fluorescence were both significantly dependent on the light treatment (ANOVA—size: n=24, F=8.4, p=0.005; fluorescence: n=24, F=26.1, p<0.001). The diurnal increase in cell volume was significantly lower, whereas the fluorescence was significantly higher at 10% of ambient light intensity than at 30% or 60% (Tukey post hoc tests). Differences in cells size and fluorescence between the different treatments were most pronounced for the cluster of picoeukaryotes, but were not observed for *Synechococcus* cells (data not shown).

At all three light intensities, clear diel patterns were observed in the polysaccharide fraction of the water-extractable carbohydrates (Fig. 8). The diurnal build-up of polysaccharides was significantly influenced by the light treatment (ANOVA: n=22, F=14.6, p=0.001) and significantly lower at 10% than at 30% or 60% of the ambient PAR (Tukey post hoc test). The Chl *a*-normalized net diurnal polysaccharide production rate was also significantly influenced by the light treatment (ANOVA: n=22, F=6.8, p=0.01) and significantly lower at 10% (Tukey post hoc test). On days 12 and 16, data were collected separately for the >10 μm phytoplankton-size fraction. Polysaccharides in >10 μm phytoplankton accounted for 20–28% of the polysaccharide concentration at the end of the light period on day 12 and 44–50% on day 16. Chl *a* in >10 μm phytoplankton was not determined; thus, no Chl *a*-normalized production rates could be calculated for this fraction.

The data on total Chl *a*-normalized polysaccharide production rates were used for the construction of tentative polysaccharide production vs. irradiance curves, admittedly based on a limited number of light intensities (Fig. 9). For the last three experi-

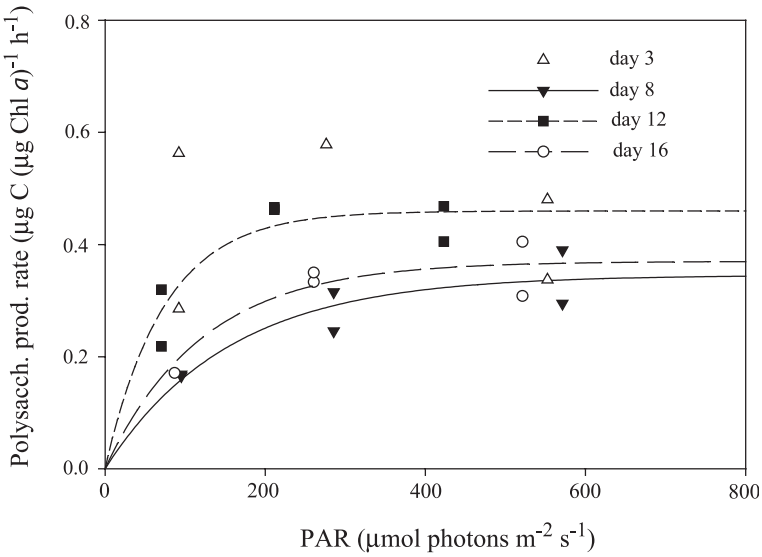

Fig. 9. The relationship between Chl *a*-normalized polysaccharide production rate and average diurnal irradiance for deck incubations with phytoplankton sampled inside the patch 3, 8, 12 and 16 days after the first Fe release. Symbols are explained in the legend. Data were fitted with a model identical to the photosynthesis–irradiance model of Webb et al. (1974). The fit for day 3 was omitted since r^2 was low.

Table 3
Parameters and regression coefficient of the polysaccharide production–irradiance curves (see Fig. 9)

	Day 3	Day 8	Day 12	Day 16
P^*_m (μg C [μg Chl a]$^{-1}$ h^{-1})	0.47	0.35	0.46	0.37
E_k (μmol photons m^{-2} s^{-1})	37.2	156.8	74.2	123.3
α^* (P^*_m/E_k)	0.0125	0.0022	0.0062	0.0030
r^2 (n=6)	0.03	0.81	0.80	0.81

ments, P^*_m varied between 0.35 and 0.46 μg C [μg Chl a]$^{-1}$ h^{-1}, α^* between 0.0022 and 0.0062 μg C [μg Chl a]$^{-1}$ h^{-1} (μmol m^{-2} s^{-1})$^{-1}$, and E_k between 74 and 157 μmol m^{-2} s^{-1} (Table 3). The r^2 of the model fit was extremely low (0.03) for the first experiment (day 3) and the parameters of this fit are not further discussed.

5. Discussion

The mesoscale iron enrichment experiment in the Southern Ocean, EisenEx/CARUSO, induced a remarkable phytoplankton bloom in the austral spring. The bloom has been followed for 3 weeks. The amount of water-extractable carbohydrates in the particulate fraction was up to two times higher inside the patch compared to the surrounding waters, thus providing the first evidence of enhanced carbohydrate production by phytoplankton in response to iron fertilization.

The shift in the size-fractionated carbohydrate measurements towards the largest size fraction (>10 μm) agrees with the observed shift in chlorophyll *a* towards the >20 μm size fraction (Gervais et al., 2002) and the increase in the relative abundance of large diatom species, i.e., *Pseudonitschzia* sp. and *Fragilariopsis* sp. (Assmy and Henjes, unpublished data). The shift towards large diatoms is typical for iron enrichment experiments and has been observed during Ironex II (Coale et al., 1996) and SOIREE (Gall et al., 2001a). In all experiments, this shift became apparent only after at least a week.

The increase in F_v/F_m and decrease in σPSII and t-Q_a in response to Fe release are typical biophysical signatures of iron-limited phytoplankton (Greene et al., 1991, 1992). Together with the increased rates of net diurnal Chl *a*-specific polysaccharide production (Table 2), this clearly indicates the iron-enhanced efficiency of photosynthetic processes. This supports the findings of laboratory experiments and a theoretical model that the photosynthetic apparatus is the primary target of iron limitation (Flynn and Hipkin, 1999; Milligan and Harrison, 2000; Davey and Geider, 2001). Not only the diurnal production but also the nocturnal consumption of polysaccharides increased and thus diel dynamics became much more pronounced upon Fe-enrichment (Fig. 6). All together, these are indicative of enhanced phytoplankton growth.

The flow cytometry revealed the increase in the cell size of pico- and <10 μm phytoplankton inside the patch (Fig. 5), which is a commonly observed response of iron-limited phytoplankton cells (Doucette and Harisson, 1991; Muggli et al., 1996; Maldonado and Price, 1996; Stefels and Van Leeuwe, 1998). The enhanced diel dynamics in the volume of these cells (Fig. 5) may be directly related to the dynamics in polysaccharide production, which has been suggested by Claustre and Gostan (1987).

Because flow-cytometrically derived fluorescence per cell is a good proxy of Chl *a* per cell (Sosik et al., 1989), the strong diel dynamics in cellular fluorescence of pico- and nanophytoplankton inside the patch (Fig. 5G–L) can be interpreted as the enhanced dynamics in cellular Chl *a* content. Our fluorescence measurements indicated that the average cellular Chl *a* content of pico- and nanophytoplankton had both increased considerably (Fig. 5), which is in agreement with laboratory experiments (Greene et al., 1991, 1992). An iron-stimulated increase in average cellular fluorescence and cell size for the clusters of *Synechococcus*, and pico- and nanophytoplankton was previously observed in the equatorial Pacific during IronEx II (Cavender-Bares et al., 1999). In contrast, at our site, fluorescence and size of *Synechococcus* cells did not increase, implying that this group of phytoplankton was not Fe-limited.

The amounts of water-extractable monosaccharides and polysaccharides and their ratios in the euphotic zone were similar to the measurements at the Antarctic Polar Front during the austral autumn of 1999 (Van Oijen et al., 2003). The low polysaccharide to monosaccharide ratio we measured in >10 μm phytoplankton compared to <10 μm phytoplankton

could be related to the regulation of the osmotic pressure in the cells. This pressure is highly influenced by the monosaccharide but little by the polysaccharide concentration in the cell. Hence, large cells need relatively more monosaccharides to maintain osmotic pressure than small cells.

The contribution of water-extractable polysaccharides to the total carbohydrate pool is comparable to the contribution of dilute acid-soluble carbohydrates to the total pool in a Norwegian Fjord (Granum and Myklestad, 2002). Cell wall polysaccharides constitute an important part of non-water-extractable carbohydrates and their production is not as directly light dependent as that of water-extractable polysaccharides. This likely caused the observed decrease in the contribution of polysaccharides with depth (Fig. 4).

The high variability in the irradiance regime during the fertilization experiment most likely influenced the temporal evolution of carbohydrates inside the patch. First, the high variations in daily surface PAR (from 12 to 55 mol photons m^{-2} day^{-1}) likely caused high variations in daily carbohydrate production. Second, the deck incubations revealed that the day–night cycle in incident PAR induces strong diel variations in carbohydrate concentration. Finally, the storms influenced the vertical distributions of phytoplankton and, hence, the effective irradiance exposure and carbohydrate production.

The deck incubations showed that polysaccharide production by phytoplankton was light-limited at 10% of full sunlight irradiance. Light limitation at this irradiance was also evident from an increase in cellular fluorescence and thus pigment content, a known sign of low light adapted cells (Falkowski, 1980). Because of dramatic increase in phytoplankton biomass, the depth at which PAR was 10% of near-surface PAR decreased from 33 to 20 m during the experiment (Gervais et al., 2002). During the second half of the experiment, as much as 60% to 80% of the upper mixed layer exhibited light conditions sub-optimal for carbohydrate production. This implies that the light limitation not only led to low production but likely also led to extra consumption of carbohydrates by phytoplankton in deep layers (Van Oijen et al., 2003).

We compared the parameters of our tentative polysaccharide production vs. irradiance curves to the parameters estimated by ^{14}C incubations under artificial light on the same days (Gervais et al., 2002). It should be noted that our incubation period was longer, 16 vs. 4 h, which could lead to a lower estimation of the rate of polysaccharide production due to respiration. The measured maximum net diurnal polysaccharide production rates were $30\pm5\%$ (n=3) of the total carbon incorporation rates estimated by ^{14}C incubations. This percentage is within the range of estimated contributions of the 'low molecular weight metabolites' pool to the total diurnal carbon incorporation in ^{14}C experiments with natural populations and monocultures of Southern Ocean phytoplankton (Smith and Morris, 1980; Mathot et al., 1992; Thomas and Gleitz, 1993). The values of the light saturation parameter E_k for the diurnal carbohydrate production were within the range of E_k values measured for total carbon incorporation during the fertilization experiment (Gervais et al., 2002) and during other cruises in the Southern Ocean (Mathot et al., 1992; Jochem et al., 1995; Bracher et al., 1999). Notably, little changes were observed during the course of the fertilization experiment in the production rates in the series of type B deck incubations, in agreement with the little changes in the total Chl a-specific ^{14}C fixation measured by Gervais et al. (2002).

Polysaccharide concentrations at the end of the light period during the deck incubations were much higher than the values measured in situ. This was likely because of the higher light availability during deck incubations than in situ. Moreover, in situ samples were often taken before the end of the day. Another possible explanation for the discrepancy is the absence of large grazers (copepods) in the deck incubations and their high abundance in situ (Verity, unpublished results).

The threefold decrease in the ratio of water-extractable carbohydrate to Chl a during the course of the fertilization experiment can be explained, in part, by a decrease in the cellular carbohydrate production (or even consumption) and, in part, by an increase in the cellular Chl a content. As evidenced by the deck incubations, it is likely that carbohydrate production decreased because of the decrease in average light availability during the course of the experiment. The deck incubations also showed that an increase in cellular Chl a content was likely, both as a physiological adaptation to the low average light

intensities and as a response to Fe fertilization (see above). In addition, the decrease in the ratio of carbohydrate to Chl *a* might be related to the shift in species composition. The ratio could be different between species, for instance due to a stronger "package-effect" of Chl *a* in larger cells (Raven, 1999). Unfortunately, no ratios of carbohydrate to Chl *a* could be calculated for the separate size fractions, because Chl *a* was size-fractionated in a different way. Notably, the Fe addition was not the most important factor explaining the decrease in the ratio of water-extractable carbohydrate to Chl *a*, since a similar decrease was observed in in-patch and out-patch samples.

The little difference in the carbohydrate to Chl *a* ratios between inside and outside the patch seems to contradict the increase in the net diurnal Chl *a*-specific carbohydrate production rates in response to iron fertilization recorded in the deck incubations. However, the nocturnal consumption of carbohydrates also increased and, consequently, there was no significant difference in the daily average of the Chl *a*-specific carbohydrate concentration between in-patch and out-patch samples.

The water-extractable carbohydrates of the particulate fraction may have included exopolysaccharides (Hama and Handa, 1992). In fact, part of the produced carbohydrates could be transformed to the dissolved organic carbon pool (Biersmith and Benner, 1998). This would enhance the trophic link between phytoplankton production and bacterial production (e.g., Fajon et al., 1999). In addition, carbohydrates have been found to be important in the formation of transparent exopolymer particles that has far-reaching implications for the aggregation of diatoms during blooms and the export of organic material out of the euphotic zone (Mopper et al., 1995; Passow, 2002). Future research should focus on linking the effects of iron on carbohydrate production by phytoplankton with changes in the export of both particulate and dissolved organic carbon. Dissolved organic carbon may contribute significantly to the total export of carbon in the Southern Ocean, especially in regions where deep water formation occurs (Schlitzer, 2002).

For logistic reasons, it was not possible to take in situ samples frequently and at pre-determined times of the day. Given the strong diel dynamics in the carbohydrate concentration and cell size and fluorescence, such sampling strategy would provide insight into the high-resolution temporal patterns of carbohydrate concentration in relation to iron availability in situ. Such a dataset will provide a basis for modeling dynamics in carbohydrates, for instance, with the ecological model SWAMCO (Lancelot et al., 2000) which already identifies several intracellular pools including the pool of storage carbohydrates. This could also be an important tool to investigate if carbohydrate consumption in deeper water layers is a mechanism underlying the observed patterns in the field.

To our knowledge, this is the first report of the phytoplankton carbohydrate response to in situ Fe fertilization. By combining in situ sampling and 24-h deck incubations, we have established that carbohydrate production by phytoplankton increases in response to Fe addition. This increase is due to both an increase in the abundance of large diatoms and physiological stimulation of the resident phytoplankton. Interestingly, even after iron addition, the diurnal carbohydrate production was limited by light availability in a large part of the deeply mixed water column. The results clearly suggest that both iron and light are the key factors controlling the formation and magnitude of phytoplankton blooms in the Southern Ocean.

Acknowledgements

We acknowledge the captain and crew of RV Polarstern, the chief scientist V. Smetacek and colleagues (phytoplankton cell counts), A. Watson and colleagues (SF_6 dosage and measurements), V. Strass and colleagues (CTD measurements and sampling, physical hydrography), U. Riebesell and colleagues (Chl *a* measurements) and C. Hartmann and colleagues (nutrient analyses). Special thanks are due to F. Gervais for data on mixing depth and euphotic depth. R. Koeman provided cell counts on preserved samples. P. Croot, P. Laan and K. Timmermans assisted during deck operations, E. Top in design and construction of the deck incubator. We thank W. Gieskes for valuable comments on the manuscript. Our research was supported by the European Commission's Environmental and Climate Research Programme—CARbon dioxide Uptake by

the Southern Ocean (CARUSO)—(EC contract no. ENV4-CT 97-0472). MYG was supported by NSF.

References

Arar, E.J., Collins, G.B., 1992. Method 445.0-in vitro determination of Chl *a* and phaeophytin a in marine and freshwater phytoplankton by fluorescence. US EPA Methods for the Determination of Chemical Substances in Marine and Estuarine Environmental Samples. U.S. Environmental Protection Agency, pp. 1–14.

Biersmith, A., Benner, R., 1998. Carbohydrates in phytoplankton and freshly produced dissolved organic matter. Marine Chemistry 63, 131–144.

Boyd, P.W., Abraham, E.R., 2001. Iron-mediated changes in phytoplankton photosynthetic competence during SOIREE. Deep-Sea Research. Part 2. Topical Studies in Oceanography 48, 2529–2550.

Boyd, P.W., et al., 2000. A mesoscale phytoplankton bloom in the polar Southern Ocean stimulated by iron fertilization. Nature 407, 695–702.

Bracher, A.U., Kroon, B.-M.A., Lucas, M.I., 1999. Primary production, physiological state and composition of phytoplankton in the Atlantic Sector of the Southern Ocean. Marine Ecology. Progress Series 190, 1–16.

Buma, A.G.J., De Baar, H.J.W., Nolting, R.F., Van Bennekom, A.J., 1991. Metal enrichment experiments in the Weddell–Scotia Seas: effects of iron and manganese on various plankton communities. Limnology and Oceanography 36, 1865–1878.

Cavender-Bares, K.K., Mann, E.L., Chisholm, S.W., Ondrusek, M.E., Bidigare, R.R., 1999. Differential response of equatorial Pacific phytoplankton to iron fertilization. Limnology and Oceanography 44, 237–246.

Claustre, H., Gostan, J., 1987. Adaptation of biochemical composition and cell size to irradiance in two microalgae: possible ecological implications. Marine Ecology. Progress Series 40, 167–174.

Coale, K.H., et al., 1996. A massive phytoplankton bloom induced by an ecosystem-scale iron fertilization experiment in the equatorial Pacific Ocean. Nature 383, 495–508.

Croot, P., et al., 2001. Iron fertilisation in the Atlantic sector of the Southern Ocean. Berichte zur Polarforschung 400, 133–148.

Cuhel, R.L., Ortner, P.B., Lean, D.R.S., 1984. Night synthesis of protein by algae. Limnology and Oceanography 29, 731–744.

Davey, M.S., Geider, R.J., 2001. Impact of iron limitation on the photosynthetic apparatus of the diatom *Chaetoceros muelleri* (Baccillariophyceae). Journal of Phycology 37, 987–1000.

De Baar, H.J.W., Buma, A.G.J., Nolting, R.F., Cadée, G.C., Jacques, G., Tréguer, P., 1990. On iron limitation of the Southern Ocean: experimental observations in the Weddell and Scotia Seas. Marine Ecology. Progress Series 65, 105–122.

Doucette, G.J., Harisson, P.J., 1991. Aspects of iron and nitrogen nutrition in the red tide dinoflagellate *Gymnodinium sanguineum*: I. Effects of iron depletion and nitrogen source on biochemical composition. Marine Biology 110, 165–173.

Dubois, M., Gilles, K.A., Hamilton, J.K., Rebers, P.A., Smith, F., 1956. Colorimetric method for determination of sugars and related substances. Analytical Chemistry 28, 350–356.

Fajon, C., Cauwet, G., Lebaron, P., Terzic, S., Ahel, M., Malej, A., Mozetic, P., Turk, V., 1999. The accumulation and release of polysaccharides by planktonic cells and the subsequent bacterial response during a controlled experiment. FEMS Microbiology, Ecology 29, 351–363.

Falkowski, P.G., 1980. Light-shade adaptation in marine phytoplankton. In: Falkowski, P.G. (Ed.), Primary Productivity in the Sea. Plenum Press, New York, pp. 99–119.

Flynn, K.J., Hipkin, C.R., 1999. Interactions between iron, light, ammonium, and nitrate: insights from the construction of a dynamic model of algal physiology. Journal of Phycology 35, 1171–1190.

Gall, M.P., Boyd, P.W., Hall, J., Safi, K.A., Chang, H., 2001a. Phytoplankton processes: Part 1. Community structure during the Southern Ocean Iron RElease Experiment (SOIREE). Deep-Sea Research: Part 2. Topical Studies in Oceanography 48, 2551–2570.

Gall, M.P., Strzepek, R., Maldonado, M., Boyd, P.W., 2001b. Phytoplankton processes: Part 2. Rates of primary production and factors controlling algal growth during the Southern Ocean Iron RElease Experiment (SOIREE). Deep-Sea Research: Part 2. Topical Studies in Oceanography 48, 2571–2590.

Geider, R.J., La Roche, J., 1994. The role of iron in phytoplankton photosynthesis and the potential for iron-limitation of primary productivity in the sea. Photosynthesis Research 39, 275–301.

Gervais, F., Riebesell, U., Gorbunov, M.Y., 2002. Changes in size-fractionated primary productivity and chlorophyll *a* in response to iron fertilization in the Southern Polar Frontal Zone. Limnology and Oceanography 47, 1324–1335.

Granum, E., Myklestad, S.M., 2001. Mobilization of beta-1,3-glucan and biosynthesis of amino acids induced by NH_4^+ addition to N-limited cells of the marine diatom *Skeletonema costatum* (Bacillariophyceae). Journal of Phycology 37, 772–782.

Granum, E., Myklestad, S.M., 2002. A simple and combined method for determination of β-1,3-glucan and cell wall polysaccharides in diatoms. Hydrobiologia 477, 155–161.

Greene, R.M., Geider, R.J., Falkowski, P.G., 1991. Effect of iron limitation on photosynthesis in a marine diatom. Limnology and Oceanography 36, 1772–1782.

Greene, R.M., Geider, R.J., Kolber, Z., Falkowski, P.G., 1992. Iron-induced changes in light harvesting and photochemical energy conversion processes in eukaryotic marine algae. Plant Physiology 100, 565–575.

Hama, J., Handa, N., 1992. Diel variation of water-extractable carbohydrate composition of natural phytoplankton populations in Kinu-ura Bay. Journal of Experimental Marine Biology and Ecology 162, 159–176.

Hitchcock, G.L., 1980. Diel variation in chlorophyll *a*, carbohydrate and protein content of the marine diatom *Skeletonema costatum*. Marine Biology 57, 271–278.

Jochem, F.J., Mathot, S., Quéguiner, B., 1995. Size-fractionated primary production in the open Southern Ocean in austral spring. Polar Biology 15, 381–392.

Kolber, Z.S., Prasil, O., Falkowski, P.G., 1998. Measurements of variable chlorophyll fluorescence using fast repetition rate techniques: defining methodology and experimental protocols. Biochimica et Biophysica Acta 1367, 88–106.

Lancelot, C., Hannon, E., Becquevort, S., Veth, C., De Baar, H.J.W., 2000. Modeling phytoplankton blooms and carbon export production in the Southern Ocean: dominant controls by light and iron in the Atlantic sector in Austral spring 1992. Deep-Sea Research: Part 1. Oceanographic Research Papers 47, 1621–1662.

Maldonado, M.T., Price, N.M., 1996. Influence of N substrate on Fe requirements of marine centric diatoms. Marine Ecology. Progress Series 141, 161–172.

Martin, J.H., Fitzwater, S.E., Gordon, R.M., 1990. Iron deficiency limits phytoplankton growth in Antarctic waters. Global Biogeochemical Cycles 4, 5–12.

Martin, J.H., et al., 1994. Testing the iron hypothesis in ecosystems of the equatorial Pacific Ocean. Nature 371, 123–129.

Mathot, S., Dandois, J.-M., Lancelot, C., 1992. Gross and net primary production in the Scotia–Wedell Sea sector of the Southern Ocean during spring 1988. Polar Biology 12, 321–332.

Milligan, A.J., Harrison, P.J., 2000. Effects of non-steady-state iron limitation on nitrogen assimilatory enzymes in the marine diatom *Thalassiosira weissflogii* (Bacillariophyceae). Journal of Phycology 36, 78–86.

Mitchell, B.G., Brody, E.A., Holm-Hansen, O., McClain, C., Bishop, J., 1991. Light limitation of phytoplankton biomass and macronutrient utilization in the Southern Ocean. Limnology and Oceanography 36, 1662–1677.

Mopper, K., Zhou, J., Ramana Sr., K., Passow, U., Dam, H.G., Drapeau, D.T., 1995. The role of surface-active carbohydrates in the flocculation of a diatom bloom in a mesocosm. Deep-Sea Research: Part 2. Topical Studies in Oceanography 42, 47–73.

Muggli, D.L., Lecourt, M., Harrison, P.J., 1996. Effects of iron and nitrogen source on the sinking rate, physiology and metal composition of an oceanic diatom from the subarctic Pacific. Marine Ecology. Progress Series 132, 215–227.

Myklestad, S.M., Skånøy, E., Hestmann, S., 1997. A sensitive and rapid method for analysis of dissolved mono- and polysaccharides in seawater. Marine Chemistry 56, 279–286.

Nelson, D.M., Smith Jr., W.O., 1991. Sverdrup revisited: critical depths, maximum chlorophyll levels, and the control of the Southern Ocean productivity by the irradiance-mixing regime. Limnology and Oceanography 36, 1650–1661.

Obata, H., Karatani, H., Nakayama, E., 1993. Automated determination of iron in seawater by chelating resin concentration and chemiluminescence detection. Analytical Chemistry 65, 1524–1528.

Obata, H., Karatani, H., Matsui, M., Nakayama, E., 1997. Fundamental studies for chemical speciation of iron in seawater with an improved analytical method. Marine Chemistry 56, 97–106.

Passow, U., 2002. Transparent exopolymer particles (TEP) in aquatic environments. Progress in Oceanography 55, 287–333.

Raven, J.A., 1999. Picophytoplankton. Progress in Phycological Research 13, 33–106.

Salisbury, F.B., Ross, C.W., 1992. Plant Physiology. Wadsworth Publishing, Belmont, CA.

Schlitzer, R., 2002. Carbon export fluxes in the Southern Ocean: results from inverse modeling and comparison with satellite-based estimates. Deep-Sea Research: Part 2. Topical Studies in Oceanography 49, 1623–1644.

Smith, A.E., Morris, I., 1980. Pathways of carbon assimilation in phytoplankton from the Antarctic Ocean. Limnology and Oceanography 25, 865–872.

Sosik, H.M., Chisholm, S.W., Olson, R.J., 1989. Chlorophyll fluorescence from single cells: interpretation of flow cytometric signals. Limnology and Oceanography 34, 1749–1761.

Stefels, J., Van Leeuwe, M.A., 1998. Effects of iron and light stress on the biochemical composition of Antarctic *Phaeocystis* sp. (Prymnesiophyceae): I. Intracellular DMSP concentrations. Journal of Phycology 34, 486–495.

Strass, V., Leach, H., Cisewski, B., Gonzalez, S., Post, J., Da Silva Duarte, V., Trumm, F., 2001. The physical setting of the Southern Ocean iron fertilisation experiment. Berichte zur Polarforschung 400, 94–130.

Thomas, D.N., Gleitz, M., 1993. Allocation of photoassimilated carbon into major algal metabolite fractions: variation between two diatom species isolated from the Weddell Sea (Antarctica). Polar Biology 13, 281–286.

Underwood, A.J., 1997. Experiments in Ecology: Their Logical Design and Interpretation Using Analysis of Variance. University Press, Cambridge, UK.

Van Leeuwe, M.A., De Baar, H.J.W., 2000. Photoacclimation by the Antarctic flagellate *Pyramimonas* sp. (Prasinophyceae) in response to iron limitation. European Journal of Phycology 35, 295–303.

Van Leeuwe, M.A., Scharek, R., De Baar, H.J.W., De Jong, J.T.M., Goeyens, L., 1997. Iron enrichment experiments in the Southern Ocean: physiological responses of plankton communities. Deep-Sea Research: Part 2. Topical Studies in Oceanography 44, 189–207.

Van Oijen, T., Van Leeuwe, M.A., Gieskes, W.W.C., 2003. Variation of particulate carbohydrate pools over time and depth in a diatom-dominated plankton community at the Antarctic Polar Front. Polar Biology 26, 195–201.

Watson, A., Messias, M.-J., Goldson, L., Skjelvan, I., Nightingale, P., Liddicoat, M., 2001. SF_6 measurements on EisenEx. Berichte zur Polarforschung 400, 76–79.

Webb, W.L., Newton, M., Starr, D., 1974. Carbon dioxide exchange of *Alnus rubra*: a mathematical model. Oecologia 17, 281–291.